Design, synthesis and evaluation of peptide inhibitors of *Mycobacterium tuberculosis* ribonucleotide reductase

JOHANNA NURBO,[a] ANNETTE K. ROOS,[b] DANIEL MUTHAS,[a] ERIK WAHLSTRÖM,[b] DANIEL J. ERICSSON,[b] TORBJÖRN LUNDSTEDT,[a,c] TORSTEN UNGE[b]* and ANDERS KARLÉN[a]*

[a] Department of Medicinal Chemistry, Organic Pharmaceutical Chemistry, BMC, Uppsala University, Box 574, SE-751 23 Uppsala, Sweden
[b] Department of Cell and Molecular Biology, Structural Biology, BMC, Uppsala University, Box 596, SE-751 24 Uppsala, Sweden
[c] AcurePharma AB, Ulleråkersvägen 38, SE-756 43 Uppsala, Sweden

Abstract: *Mycobacterium tuberculosis* ribonucleotide reductase (RNR) is a potential target for new antitubercular drugs. Herein we describe the synthesis and evaluation of peptide inhibitors of RNR derived from the *C*-terminus of the small subunit of *M. tuberculosis* RNR. An *N*-terminal truncation, an alanine scan and a novel statistical molecular design (SMD) approach based on the heptapeptide Ac-Glu-Asp-Asp-Asp-Trp-Asp-Phe-OH were applied in this study. The alanine scan showed that Trp5 and Phe7 were important for inhibitory potency. A quantitative structure relationship (QSAR) model was developed based on the synthesized peptides which showed that a negative charge in positions 2, 3, and 6 is beneficial for inhibitory potency. Finally, in position 5 the model coefficients indicate that there is room for a larger side chain, as compared to Trp5. Copyright © 2007 European Peptide Society and John Wiley & Sons, Ltd.

Keywords: *Mycobacterium tuberculosis*; ribonucleotide reductase; peptide inhibitors; alanine scan; statistical molecular design; structure activity relationships; FHDoE

INTRODUCTION

Mycobacterium tuberculosis is the pathogen that causes tuberculosis. The World Health Organization estimates that overall one third of the world's population is currently infected by the bacteria and has declared tuberculosis as a global emergency [1]. Serious challenges associated with the rising epidemic are multidrug-resistance and the growing number of people co-infected with *M. tuberculosis* and human immunodeficiency virus (HIV) [2]. Today's treatment consists of extensive chemotherapy, where complementary drugs are combined and administration periods stretch over several months. Side effects, in addition to the problems associated with patients interrupting the treatment in advance, add to the seriousness of the disease and therefore there is a need for new antitubercular drugs.

Ribonucleotide reductase (RNR) catalyzes the reduction of ribonucleotides to the corresponding deoxyribonucleotides and is an essential enzyme for DNA synthesis [3]. The active enzyme is a tetramer composed of two large subunits (R1) and two small subunits (R2) [4]. R1 possesses the substrate and effector binding sites [5] while R2 harbors a tyrosine radical [6] essential for catalytic activity. The catalytic mechanism involves electron transfer between the radical in R2 and the active site in R1. The association of the subunits is therefore crucial for enzymatic activity.

RNR is a well-known target for cancer therapy and antiviral agents [7,8]. In *M. tuberculosis* the gene for the R1 subunit is encoded by *nrdE* (Rv3051c) [9] and it has been shown that *nrdF2* (Rv3048c) corresponds to the R2 subunit used by the bacterium [10]. These genes have been found to be required for optimal bacterial growth in transposon site hybridization studies [11]. Furthermore, gene knockout studies and expression analysis by Dawes and coworkers [10] have shown that *nrdE* in combination with *nrdF2* is essential for bacterial growth. Therefore, RNR may also be a promising target for development of new antitubercular drugs.

Several different approaches for inhibiting RNR have been explored [7], and one possible approach is to inhibit the association of the R1 and R2 subunits. Studies with the *E. coli* [12], mammalian [13] and herpes simplex virus (HSV) [14] RNR systems have shown that peptides corresponding to the *C*-terminal end of the R2 subunit can compete for the R2 binding site of R1 and thus inhibit RNR activity. Several structure activity studies starting from *C*-terminal peptides have appeared for mammalian and HSV RNR [15–17]. Peptides derived from the *C*-terminal end of the *M. tuberculosis* R2 subunit have also been investigated (Figure 1). However, for *M. tuberculosis* only a handful of analogous have been tested for their ability to inhibit RNR [18]. For example, the *C*-terminal heptapeptide, Glu-Asp-Asp-Asp-Trp-Asp-Phe-OH, had an IC$_{50}$ value of 100 μM and the *N*-terminally acetylated analog,

*Correspondence to: T. Unge, Department of Cell and Molecular Biology, Structural Biology, BMC, Uppsala University, Box 596, SE-751 24 Uppsala, Sweden; e-mail: torsten.unge@icm.uu.se
A. Karlén, Department of Medicinal Chemistry, Organic Pharmaceutical Chemistry, BMC, Uppsala University, Box 574, SE-751 23 Uppsala, Sweden; e-mail: anders.karlen@orgfarm.uu.se

Ac-Glu-Asp-Asp-Asp-Trp-Asp-Phe-OH (**1**) was five times more potent with an IC_{50} value of 20 µM. In that study it was also shown that removal of the *N*-terminal Glu residue from **1** still resulted in an IC_{50} value of 60 µM corresponding to a three-fold loss in potency [18]. Altogether, RNR seemed to us to be a promising antitubercular target which prompted us to begin a study of the structure activity relationships (SAR) of peptide **1**.

MATERIALS AND METHODS

General Methods

LC-MS was performed on a Gilson–Finnigan AQA system (Gilson, Middletown, WI, USA and Thermo Electron, Woburn, MA, USA) in ESI mode using a Chromolith SpeedROD RP-18e 4.6×50 mm column (Merck) and a CH_3CN/H_2O linear gradient with 0.05% HCOOH. Analytical RP–HPLC was carried out on an ACE 5 Phenyl column (4.6×50 mm) and a CH_3CN/H_2O linear gradient with 0.1% TFA, a YMC 5 ODS–AQ column (4.6×50 mm) and a CH_3CN/H_2O linear gradient with 0.1% TFA or an ACE 5 C18 column (4.6×50 mm) and a CH_3CN/H_2O linear gradient with 0.25 mM NH_4OAc, pH 6.3 at a flow rate of 2 ml/min and detection at 220 nm. Amino acid analysis was performed at the Department of Biochemistry, Uppsala University, Sweden. Samples were hydrolyzed with 6 M HCl at 110 °C for 24 h and analyzed with ninhydrin detection. ^1H NMR was obtained after desalting the peptide using RP-HPLC with a CH_3CN/H_2O linear gradient with 0.1% TFA. The spectra were recorded on a Varian Mercury plus spectrometer at 400 Hz. Chemical shifts are reported as δ values (ppm) referenced to δ 2.50 ppm for DMSO-d_6. HRMS was obtained on a Micromass Q-Tof2 mass spectrometer equipped with an electrospray ion source. DNA sequence analysis was performed at Uppsala Genome Center, Rudbeck Laboratory, Uppsala University, Sweden.

Solid-phase Peptide Synthesis

Peptides **1**–**27** were prepared with a Symphony instrument (Protein Technologies Inc., Tucson, AZ, USA). The synthesis of the peptides was accomplished on a 100-µmol scale using Fmoc/tBu-protection. The starting polymer was Fmoc-Phe-Wang resin (Calbiochem–Novabiochem, Läufelfingen, Switzerland) for peptide **1**–**10**, H-Phe-2-Chlorotrityl resin (Iris Biotech GmbH, Marktredwitz, Germany), for peptide **13, 15, 16, 21**–**23**, **25** and **27**. The remaining starting polymers were prepared from 2-Cl-tritylchloride resin (Alexis Corporation, Lausen, Switzerland) as described in the literature [19]. Amino acid derivatives were obtained from Alexis Corporation,

AnaSpec Inc. (San Jose, CA, USA), Calbiochem–Novabiochem, Iris Biotech GmbH, Neosystem (Strasbourg, France), PepTech Corporation (Burlington, MA, USA) and Senn Chemicals (Dielsdorf, Switzerland). Amino acids with the following side chain protection were used: Asn(Trt), Asp(O*t*-Bu), Dab(Boc), Dap(Boc), Gln(Trt), Glu(O*t*-Bu), Orn(Boc), Ser(O*t*-Bu), Thr(O*t*-Bu), Trp(Boc).

The Fmoc group was removed by treatment with 20% piperidine in dimethyl formamide (DMF) for 2×5 min. Coupling of the amino acids was performed in DMF using *N*-[(1H-benzotriazole-1-yl)-(dimethylamino)-methylene]-*N*-methylmethanaminium hexafluorophosphate *N*-oxide (HBTU) (Iris Biotech GmbH) in the presence of *N*-methyl morpholine. Double couplings (2×30 min) were used for the common amino acids, manual addition and single couplings (60 min) for the unusual amino acids. Free amino groups remaining after each coupling cycle were capped by addition of 20% acetic anhydride in DMF to the coupling mixture and allowed to react for 5 min. After completion of the sequence, the Fmoc group was removed and the *N*-terminal was acetylated by addition of 20% acetic anhydride in DMF allowing the reaction to proceed for 2×15 min. The resin was washed with DMF and DCM and dried in a stream of nitrogen and *in vacuo*.

Approximately 150 mg of the resin was treated with 95% aqueous TFA (2 ml) and triethylsilane (100 µl) for 1.5 h. The mixture was filtered through a plug of glass wool in a Pasteur pipet, and the resin was washed with TFA (0.3 ml). The TFA was partially evaporated and the product was precipitated by the addition of ether (12 ml). The precipitate was collected by centrifugation, washed with ether (3×10 ml) and dried.

Aliqouts of the crude peptides, approximately 25 mg, were purified using one of the following systems. Peptide **1, 2, 5**–**10, 12**–**15** and **17**–**27** were purified by preparative RP-HPLC on an ACE-Phenyl, 5 µm, (21.2×150 mm) column, a Vydac, 10 µm, C18 column (22×250 mm) or a Combi HT SB-C8, 5 µm, (21.2×50 mm) column using a CH_3CN/H_2O linear gradient with 0.25 mM NH_4OAc, pH 6.3. Peptides **11** and **16** were purified by ion-exchange chromatography on a Dymo AQ4 column using 0.025–2 M NH_4OAc pH 6.5. Peptides **3** and **4** were purified by preparative RP-HPLC on an ACE-Phenyl, 5 µm, (21.2×150 mm) column using a CH_3CN/H_2O linear gradient with 0.1% TFA. Selected fractions were pooled and lyophilized. The peptides were analyzed by LC-MS and by two different analytical RP-HPLC systems. The peptide content was determined by amino acid analysis. Analytical data, yields, and purity determinations of the peptides are shown in Tables 1 and 2.

Spectroscopic Characterization of Ac-Glu-Asp-Asp-Asp-Trp-Asp-Phe-OH (1)

^1H NMR (DMSO-d_6) δ: 12.37 (br s, 6H), 10.71 (d, $J = 2.3$ Hz, 1H), 8.21 (d, $J = 7.5$ Hz, 1H), 8.12 (d, $J = 7.8$ Hz, 1H), 8.07 (d, $J = 7.4$ Hz, 1H), 8.04 (d, $J = 7.7$ Hz, 1H), 8.03 (d, $J = 7.7$ Hz, 1H), 7.82 (d, $J = 7.9$ Hz, 1H), 7.79 (d, $J = 7.7$ Hz, 1H), 7.55 (br d, $J = 7.9$ Hz, 1H), 7.31 (br d, $J = 8.1$ Hz, 1H), 7.27–7.16 (m, 5H), 7.14 (d, $J = 2.3$ Hz, 1H), 7.04 (ddd, $J = 1.3, 7.0, 8.1$ Hz, 1H), 6.95 (ddd, $J = 1.2, 7.0, 7.9$ Hz, 1H), 4.59–4.48 (m, 4H), 4.43 (ddd, $J = 4.5, 7.9, 8.1$ Hz, 1H), 4.38 (ddd, $J = 5.8, 7.6, 7.7$ Hz, 1H), 4.19 (m, 1H), 3.12 (dd, $J = 4.5, 15.1$ Hz, 1H), 2.99 (dd, $J = 5.8, 13.9$ Hz, 1H), 2.92 (dd, $J = 8.1, 15.1$ Hz, 1H), 2.90 (dd, $J = 7.6, 13.9$ Hz, 1H), 2.73 (dd, $J = 4.8, 16.7$ Hz,
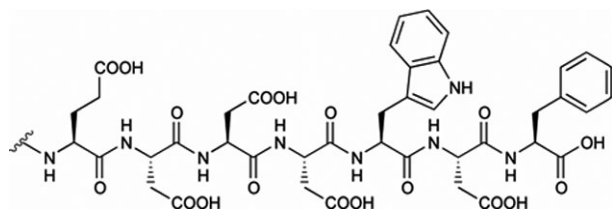

Figure 1 R2 *C*-terminal residues of *M. tuberculosis* RNR.

Table 1 Analytical data and yields of peptide **1–27**

Peptide	Amino acid analysis	$[M + H]^+$	Yield (%)[a]
1	Asp 3.59, Glu 1.02, Phe 0.98, Trp nd	983.2	13
2	Asp 3.60, Phe 1.00, Trp nd	854.3	11
3	Asp 2.63, Phe 1.00, Trp nd	739.2	19
4	Asp 1.74, Phe 1.00, Trp nd	624.1	30
5	Ala 1.02, Asp 3.66, Phe 0.98, Trp nd	925.2	25
6	Ala 0.98, Asp 2.61, Glu 1.04, Phe 0.99, Trp nd	939.2	18
7	Ala 1.00, Asp 2.63, Glu 1.03, Phe 0.97, Trp nd	939.2	20
8	Ala 1.00, Asp 3.01, Glu 1.03, Phe 0.96, Trp nd	939.1	21
9	Ala 0.99, Asp 4.03, Glu 1.02, Phe 0.96	868.2	69
10	Ala 1.02, Asp 2.63, Glu 1.04, Phe 0.94, Trp nd	939.2	8
11	Ala 1.00, Asp 3.55, Glu 1.00, Trp nd	907.1	28
12	Asp 4.00, Glu 1.00, Thi nd, Trp nd	989.4	24
13	Asp 3.00, Glu 2.03, Phe 0.98, Tyr 0.98	987.6	72
14	Asp 2.72, 3Fp nd, Glu 1.02, Thr 0.98, Trp nd	986.6	40
15	Asp 2.00, Glu 2.01, Met 0.97, Phe 1.01, Trp nd	1013.5	45
16	Asp 3.02, Ser 1.03, Met 0.97, Phe 0.98, Trp 0.67	956.5	15
17	Asp 1.73, Dap nd, Met 0.97, 2Mp nd, Thr 1.03, Trp nd	956.5	13
18	Asp 2.60, Glu 1.02, Orn 0.98, Phg nd, Trp nd	967.5	42
19	Asp 2.01, Dab nd, 3Fp nd, Orn 0.98, Thr 1.00, Tyr 0.99	948.4	27
20a	Asp 1.99, Dap nd, Glu 2.01, Nal nd, Phg nd	964.4	13
20b	Asp 1.99, Dap nd, Glu 2.00, Nal nd, Phg nd	964.5	16
21	Asp 2.63, Met 0.95, Orn 1.02, Phe 1.02, Trp nd	983.6	38
22	Glu 1.01, Ile 0.97, Orn 0.98, Phe 1.00, Ser 2.04, Trp nd	924.7	28
23	Asp 4.04, Bth nd, Dab nd, Phe 0.95	971.2	78
24	Asp 4.00, Glu 1.00, Pfp nd, Thi nd	1038.2	42
25	Asp 3.00, Dap nd, Glu 1.01, Phe 0.98, Tyr 1.01	958.6	58
26	Cit 1.00, Glu 3.99, 2Mp nd, Tyr 1.01	1084.6	34
27	Asp 2.03, Dab nd, Glu 1.00, Met 0.96, Pfp nd, Phe 0.97	1034.3	46

[a] Corrected for peptide content according to amino acid analysis.

1H), 2.68 (dd, $J = 5.7$, 16.0 Hz, 1H), 2.65 (dd, $J = 6.0$, 16.9 Hz, 1H) 2.63 (dd, $J = 6.0$, 16.6 Hz, 1H), 2.57–2.46 (m, 2H), 2.45 (dd, $J = 7.7$, 16.7 Hz, 1H), 2.39 (dd, $J = 7.7$, 16.6 Hz, 1H), 2.27–2.21 (m, 2H), 1.86 (m, 1H), 1.85 (s, 3H), 1.73 (m, 1H). HRMS (M + H⁺): 983.3258, $C_{43}H_{51}N_8O_{19}$ requires 983.3270.

Design of a Peptide Library and OPLS Analysis

A peptide library was generated employing focused hierarchical design of experiments (FHDoE) [20]. The design was performed in building block space using the individual amino acids as variables. Each amino acid was described with two components from the theoretically derived chemically intuitive z-scales (tciz) (Table 3) [20]. The first variable, tciz1 represents mainly size and tciz2 mainly reflects hydrophilicity/hydrophobicity. The covariance matrix as well as synthetic aspects, price and accessibility of amino acids guided the final selection. Building blocks were chosen from the vicinity around the amino acid residues found in the reference peptide **1** (Figure 2). In accordance with FHDoE, a substitution matrix based on a 2^{7-3} fractional factorial design (FFD) was combined with a 2^{14-10} FFD to create the design matrix used (Table 4) resulting in a library of 16 peptides. The design was augmented with the seven peptides from the classical alanine scan. The MODDE software (*MODDE*, version 6.0; Umetrics

AB, Umeå, Sweden) was used to inspect design properties, and the variables were reordered to achieve good design properties.

An orthogonal partial least squares projection to latent structure discriminant analysis (OPLS-DA) [21–23] model was developed from peptide **1** and **5–27**. Each peptide was described using the same properties as in the design step together with a qualitative charge descriptor that was added to those positions where the charge was varied, i.e. 1, 2, 3, 4, and 6. Variables were scaled to unit-variance and mean centered. All peptides with IC_{50} values below 1 mM were considered to be active (class membership $Y = 1$), whereas peptides exhibiting higher IC_{50} values were classified as inactive (class membership $Y = 0$). All OPLS-DA modeling was performed using SIMCA P+ (*SIMCA P+*, v.11.5; Umetrics AB, Umeå, Sweden). Variables showing small loading values in the predictive component were removed. The resulting model showed some nonlinearity and it was decided to add cross-terms. The cross-terms were added in a chemically intuitive way, only allowing interactions between the same type of variables. For example, the cross-term between the first position's tciz1 and other position's tciz1 were allowed, whereas no cross-terms between tciz1, tciz2 or ch variables were allowed. The model was refitted, and variables with low loadings in the predictive component were removed. Inspection of the DModX plot showed that no peptides were distant from the model, indicating that they were true members of either

Table 2 Purity of peptide **1**–**27**, determined by two different HPLC systems

Peptide	Ret. time[a]	Purity (%)[a]	Ret. time[b]	Purity (%)[b]	Peptide	Ret. time[a]	Purity (%)[a]	Ret. time[b]	Purity (%)[b]
1	8.87	100	4.85	98.6	**15**	10.63	97.9	7.61	98.9
2	8.77	99.5	5.16	98.9	**16**	9.99	97.7	9.88	100
3	8.39	99.6	6.07	97.9	**17**	11.37	95.2	11.86	99.8
4	9.05	100	7.60	99.8	**18**	7.96	99.5	6.44	99.8
5	8.95	100	5.82	96.8	**19**	8.55	99.6	9.90	98.4
6	9.05	98.6	5.93	98.2	**20a**	7.72	98.7	7.61	99.3
7	9.05	100	5.98	99.5	**20b**	9.75	100	7.94	99.3
8	9.13	100	5.89	98.9	**21**	9.81	97.7	10.33	99.6
9	4.02	97	4.69	98.3[c]	**22**	10.29	100	12.82	99.4
10	9.24	99.5	6.07	97.8	**23**	10.29	100	7.92	98.3
11	4.69	99.4	5.41	99.3[c]	**24**	9.27	100	7.11	99.3
12	8.26	100	4.05	99.0	**25**	9.07	100	8.26	98.9
13	8.33	100	5.59	99.3	**26**	10.23	97.1	10.25	100
14	9.09	100	6.92	99.9	**27**	11.55	96.9	12.57	98.4

[a] Analytical HPLC. Column: ACE 5 Phenyl, 4.6×50 mm Buffer A: 0.1% TFA in water. Buffer B: 0.09% TFA in CH_3CN. Gradient: 5–45%, 20 min. Flow rate: 2 ml/min. Detection: UV absorbance at 220 nm.
[b] Analytical HPLC. Column: ACE 5 C18, 4.6×50 mm. Buffer A: 0.25 mM NH_4OAc, pH 6.3. Buffer B: 0.25 mM NH_4OAc, pH 6.3 in 80% CH_3CN. Gradient: 5–45%, 20 min. Flow rate: 2 ml/min. Detection: UV absorbance at 220 nm.
[c] These peptides were too hydrophilic at pH 6.3 and were analyzed in the following system. Column: YMC 5 ODS-AQ, 4.6×50 mm. Buffer A: 0.1% TFA in water. Buffer B: 0.09% TFA in CH_3CN. Gradient: 0–30%, 20 min. Flow rate: 2 ml/min. Detection: UV absorbance at 220 nm.

class. The corresponding PLS-DA model was also generated in SIMCA P+ and validated using the validate model option employing 100 permutations. A Q^2 intercept of -0.214 and an R^2 intercept of 0.396 indicates the model validity. The model was further validated by dividing the 24 peptides into six external test-sets of four peptides each. New models were generated using the same descriptors as the final model and the test-sets were predicted. Only six peptides were wrongly classified, further supporting the model.

Cloning, Expression, and Purification of the Two *M. tuberculosis* RNR Subunits

R1: The sequence corresponding to the open reading frame of the Rv3051c gene was amplified by PCR from total DNA of *M. tuberculosis* strain H37Rv [9], using the high-fidelity polymerase Pfu Ultra (Stratagene, La Jolla, CA, USA) and the primers 5′-CCAACCGTCATTGCAGAG-3′ and 5′-CTACAGCATGCAGGACACGCAAC-3′. A histidine-tag was added to the *N*-terminus in a second PCR through the primer 5′-ATGGCTCATCATCATCATCATCATGGTCCAA-CCGTCATTGCAGAG-3′. The DNA fragment was ligated into the pCRT7 TOPO vector (Invitrogen, Carlsbad, CA, USA). Cloning was performed in *E. coli* TOP10F' cells (Invitrogen). The construct was verified by DNA sequence analysis.

Expression was performed in *E. coli* BL21/AI^{TM} (Invitrogen) cells in 50% LB and 50% minimal media by induction with 2 g/l L-arabinose. Cells containing overexpressed R1 were suspended in lysis buffer (50 mM sodium phosphate pH 8, 300 mM NaCl, 10 mM imidazole, 10% (v/v) glycerol) with 0.01 mg/ml RNase, 0.02 mg/ml DNase, 1 mM PMSF

Table 3 Tciz values of the amino acids included in the study

Abbrev.		tciz1	tciz2
2Mp	2-Methylphenylalanine	1.46	-0.78
3Fp	3-Fluorophenylalanine	0.83	-1.52
Ala	Alanine	-4.59	-1.03
Asn	Aspargine	-3.42	2.32
Asp	Aspartic acid	-3.46	1.49
Bth	3-Benzothienylalanine	3.03	-1.12
Cit	Citrulline	-0.76	4.08
Dab	2,4-Diaminobutyric acid	-3.39	1.49
Dap	2,3-Diaminopropionic acid	-4.17	0.60
Gln	Glutamine	-2.43	2.98
Glu	Glutamic acid	-2.53	2.21
Ile	Isoleucine	-1.16	-0.42
Met	Methionine	-1.40	0.25
Nal	3-(1-Naphtyl)alanine	3.82	-1.74
Oet	*O*-Ethyltyrosine	3.01	0.32
Omt	*O*-Methyltyrosine	1.86	0.03
Orn	Ornithine	-2.12	1.28
Pfp	Pentafluorophenylalanine	1.48	-1.30
Phe	Phenylalanine	0.35	-1.04
Phg	Phenylglycine	-0.52	-1.85
Ser	Serine	-4.30	0.50
Thi	2-Thienylalanine	-0.45	-0.80
Thr	Threonine	-3.35	0.39
Trp	Tryptophan	2.60	-0.62

and lyzed by passage through a Constant Cell Disruption System (Constant Systems Ltd, Daventry, UK) at 1.5 kBar.
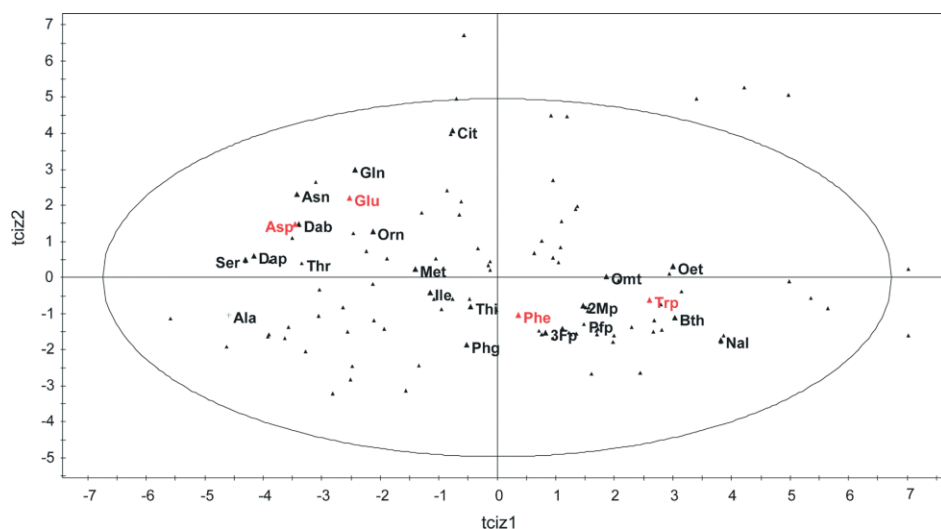
Figure 2   Scatter plot of the investigated amino acid space, showing the selected building blocks. Red dots represent the residues present in peptide **1**, and large triangles correspond to residues employed in the designed library. Alanine is also shown for comparison.

R1 was isolated with Ni-NTA agarose (Qiagen), and finally purified by size exclusion chromatography on a HiLoad 16/60 Superdex 200 column (GE Healthcare, Uppsala, Sweden). The pooled fractions (12 ml) contained R1 at a concentration of 0.3 mg/ml (A280, $\varepsilon = 0.9$). The material was precipitated with $(NH_4)_2SO_4$ and stored at 4 °C.

R2: The sequence corresponding to the active *M. tuberculosis* R2 [18] (Rv3048c, *nrdF2*) was amplified from *M. tuberculosis* DNA strain H37Rv by PCR using the primers 5′-ATGACTGGAAACGCAAAGCTAATTG-3′ and 5′-CTAGAAGTCCCAGTCATCGTC-3′, ligated to the vector pCRT7 and expressed as described above with the exception that the medium was supplemented with 33 μM of $FeCl_3$ and $FeSO_4$.

Cells containing R2 were lyzed as described above. The protein in the cleared lysate was precipitated with $(NH_4)_2SO_4$, collected by centrifugation at 39 000 × g, resuspended in 20 mM 2-(N-morpholino) ethanesulphonic acid monohydrate (MES) pH 6, 10 mM $(NH_4)_2SO_4$ and

Table 4   FHDoE design matrix used to generate a heptapeptide library of 16 peptides. Shaded cells indicate that no substitution should be made in that position

P1 tciz1	P1 tciz2	P2 tciz1	P2 tciz2	P3 tciz1	P3 tciz2	P4 tciz1	P4 tciz2	P5 tciz1	P5 tciz2	P6 tciz1	P6 tciz2	P7 tciz1	P7 tciz2
−	−	−	−	−	+	+	−	+	−	+	+	−	+
−	−	−	+	+	−	+	+	+	−	−	−	+	−
+	−	−	+	−	−	−	+	−	+	+	+	−	−
+	−	−	−	+	+	−	−	−	−	−	−	+	+
−	+	−	+	−	−	−	−	+	+	−	+	+	+
−	+	−	−	+	+	−	+	+	+	+	−	−	−
+	+	−	−	−	+	+	+	−	−	−	+	+	−
+	+	−	+	+	−	+	−	−	−	+	−	−	+
−	−	+	−	−	−	+	+	−	+	+	−	+	+
−	−	+	+	+	+	+	−	−	+	−	+	−	−
+	+	+	+	−	−	−	−	+	−	+	−	+	−
+	−	+	−	+	+	−	+	+	−	−	+	−	+
−	+	+	+	−	+	−	+	−	−	−	−	−	+
−	+	+	−	+	−	+	−	−	−	+	−	+	−
+	+	+	−	−	−	+	−	+	+	−	−	−	−
+	+	+	+	+	+	+	+	+	+	+	+	+	+

dialyzed against this buffer with a Spectra/Por (Spectrum Laboratories, Breda, Netherlands) membrane tube (MWCO of 12 000 Da). The dialysate was applied to two 1.5 ml gel beds of Q Sepharose Fast Flow (GE Healthcare). The material was eluted with 4 CV at the NaCl concentration of 0.5 M. R2 was finally purified on a HiLoad 16/60 Superdex75 (GE Healthcare) column equilibrated with 50 mM HEPES pH 7, 0.2 M Na_2SO_4. R2 eluted at an elution volume corresponding to a dimer. Homogeneous material was identified by dodecyl sulfate polyacrylamide gel electrophoresis, pooled and stored in 100 µl aliquots of ~9 mg/ml (A280, $\varepsilon = 1.6$) at $-20\,°C$.

Assay Conditions

The peptides' inhibitory capacity were estimated in the [^{3}H]CDP assay described by Engström and coworkers, [24] where the reduction of CDP is monitored. Prior to starting the enzymatic assay with RNR, the R1 subunit was activated by resuspending the $(NH_4)_2SO_4$ pellet in 0.1 M tris pH 8.3, 0.2 M Na_2SO_4, 2 M urea, 50 mM dithiothreitol (DTT) and incubating it at $22\,°C$ for 10 min. The buffer was then exchanged to 50 mM HEPES pH 7.5, 0.2 M Na_2SO_4, 10 mM DTT by multiple cycles of concentration/dilution of the protein sample in a Vivaspin 500 column (Sartorius, Goettingen, Germany). The final R1 stock solution had a concentration of 1–1.2 mg/ml. An aliquot of R2 was thawed and diluted to 1.5–1.6 mg/ml in 50 mM HEPES pH 7.5, 0.2 M Na_2SO_4.

The assay was performed in a final reaction volume of 25 µl in 19 mM MES pH 7.5, 23 mM HEPES pH 7.5, 6 mM $MgCl_2$, 16 mM Na_2SO_4, 6 mM NaF, 5 mM DTT, 3 mM ATP, and with 10 µM cold CDP and 3 µM [^{3}H]CDP (888 GBq/mmol, GE Healthcare, Little Chalfont, UK). R1 and R2 were added to a concentration of 1 and 3 µM respectively. The reaction was incubated at $37\,°C$ for 45 min. The product, dCDP, was hydrolyzed with 200 µl 0.2 M perchloric acid at $100\,°C$ for 10 min. The reaction mixture was then neutralized by addition of 70 µl 4 M KOH, centrifuged at $16\,000 × g$, and dCMP separated from CMP on a 2.7 ml, 4.5 cm high column of Dowex 50 (Fluka, Buchs, Switzerland). Samples were consistently applied in a volume of 236 µl, CMP was washed out with 42.5 ml 0.2 M HAc and dCMP eluted in a 2 ml fraction. A sample of 1 ml of the eluate was mixed with scintillation solution (Unisafe 1, Zinsser Analytic, Frankfurt, Germany) and radioactivity was measured for 1 min. Peptides were assayed for their inhibitory capacity at five concentrations (100, 200, 300, 400, 500 µM) in triplicate measurements after being dissolved in 50 mM HEPES pH 7.5 and IC_{50} values were estimated from the resulting counts per minute (cpm) values by fitting the data to Eqn (1):

$$v_I = \frac{v_0}{1 + \frac{[I]}{K_I}} \qquad (1)$$

where v_I is the velocity at the inhibitor concentration [I], v_0 the maximum velocity (without inhibitor), and K_I the inhibition constant of the inhibitor, assuming noncompetitive inhibition, as reported by Cohen and coworkers [25]. Analysis was performed using the Curve Fitting Toolbox for MATLAB (R13, The Mathworks, Natick, MA, USA). For noncompetitive inhibition $IC_{50} = K_I$ which follows from Eqn (1).

To get an estimation of the dissociation constant between the two subunits, a titration with varying concentrations of R1 and a constant concentration of R2 was performed. A K_D value was determined by nonlinear regression to Eqn (2) as described by Yang *et al.* [18], using the Curve Fitting Toolbox for MATLAB.

$$v = \frac{V_{\max}(\mathbf{R1})}{K_D + (\mathbf{R1})} \qquad (2)$$

where v is the velocity, $V_{\max}$ the maximum velocity, K_D the dissociation constant and ($\mathbf{R1}$) the free concentration of the R1 subunit calculated using Eqn (3) as,

$$(\mathbf{R1}) = 1/2 \Big\{ -(K_D + [R2]_{tot} - [R1]_{tot}) $$
$$+ \sqrt{(K_D + [R2]_{tot} - [R1]_{tot})^2 + 4 \cdot [R1]_{tot} \cdot K_D} \Big\} \quad (3)$$

where, $[R1]_{tot}$ is the total concentration of R1 ranging from 3 to 1.5 µM and $[R2]_{tot}$ the total concentration of R2, which was 0.3 µM. The data were also analyzed by including a Hill coefficient in Eqn (4):

$$v = \frac{V_{\max}(\mathbf{R1})^h}{K_{0.5}^h + (\mathbf{R1})^h} \qquad (4)$$

where, $K_{0.5}$ is the R1 concentration where $v = 1/2\,V_{\max}$ and h is the Hill coefficient. If h is larger than 1 there is positive cooperativity [26].

RESULTS AND DISCUSSION

To obtain information concerning the SAR of the heptapeptide **1**, the following strategy was applied. A series of peptides was first synthesized based on the classical approach of studying the minimal active sequence of the peptide and studying the importance of individual amino acids using an alanine scan. Based on the inhibitory potency of these peptides, the decision was made to explore the SAR of the heptapeptide in greater detail. A systematic variation of each position quickly leads to a large number of peptides to synthesize and evaluate. This together with the enormous peptide space available (20^7 using only coded amino acids) encouraged us to explore this space using the FHDoE approach [20]. One of the benefits of using statistical molecular design (SMD) is that information-rich datasets can be generated from few experiments [27–30]. By combining the results from the two series of peptides, a quantitative structure relationship (QSAR) was developed that highlights the importance of the individual amino acid positions in the peptide.

Peptide Synthesis

Peptides **1–27** were obtained by standard solid-phase methodology using Fmoc–amino acids with acid-labile side chain protecting groups. Purification by RP-HPLC or ion-exchange chromatography gave homogeneous

products. The resulting overall yields were varied between 8 and 78%, as determined by amino acid analysis. The purity of the peptides was analyzed by two different RP-HPLC systems. In all cases, the peptides were more than 95% pure. Two isomers were isolated from peptide **20**. This isomerization was presumably due to racemization of the phenylglycine residue [31]. These peptides were tested separately and are referred to as **20a** and **20b**.

Enzymatic Activity and Analysis of Peptide Inhibition

IC_{50} values for the evaluated peptides are presented in Tables 5 and 6. In the interpretation of the measurements, we assume that the cpm obtained are proportional to the initial velocities and follow Michaelis–Menten kinetics. This is reasonable since experiments showed that the activity increased linearly between 30, 45, and 60 min and only a fraction of the substrate was turned into the product. When assayed separately, R1 and R2 were both inactive with cpm values just above the background. Peptide **1** was included as a reference each time the assay was run. The IC_{50} estimates for this peptide ranged between 100 and 180 μM, which reflects the variation seen for the assay.

Activity was measured at R1 and R2 concentrations of 1 and 3 μM, respectively. These concentrations were chosen, since in this range the cpm values were more reproducible than at lower concentrations. A K_D estimation of the interaction between R1 and R2 was performed by titrating a constant concentration of R2 with a varying concentration of R1 (Figure 3). When Eqn (2), according to Yang *et al.* [18], was fitted to the data a K_D value of 0.40 ± 0.17 μM could be determined. When examining our data points for low R1 concentrations it could be seen that the curve was
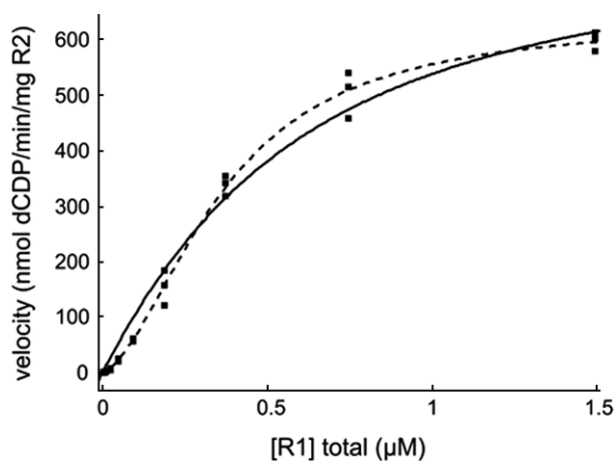

Figure 3 Estimation of the K_D for the interaction of R1 and R2 by titration of R2 (0.3 μM) with increasing concentrations of R1. The data points are shown together with the curves fitted with the two different equations, Eqns (2) and (4). The solid line shows the fit to Eqn (2) while the dashed line shows the the fit to Eqn (4), including a Hill coefficient.

slightly sigmoidal, which would suggest cooperativity. Including a Hill coefficient in the equation gave a much better correlation to the data points and resulted in a Hill coefficient of 1.4 ± 0.05, which would suggest that the system has slight positive cooperativity. From this curve the $K_{0.5}$ was determined to 0.21 ± 0.02 μM. Both curves are presented in Figure 3. The fact that positive cooperativity is observed could be explained by the RNR complex working as a dimer of dimers. Purification results show that R2 is a dimer in solution while R1 is a mixture of dimers and higher aggregates. It is not likely that both R2 subunits interact at exactly the same moment with their R1 counterparts, which would lead to the observed cooperativity.

SAR Derived from Peptide Truncation and Alanine Scan

To identify the minimal active sequence of heptapeptide **1**, we synthesized the *N*-terminally truncated analogs **2**–**4**. The IC_{50} values and relative inhibitory potencies are shown in Table 5. In accordance with previous studies by Yang and coworkers [18], it was seen that the *N*-acetylated hexapeptide (**2**) was slightly less potent as compared to **1**. The *N*-acetylated pentapeptide (**3**) retained some activity ($IC_{50} = 1110$ μM) while the *N*-acetylated tetrapeptide (**4**) lacked activity. We decided to use the most potent peptide (**1**) in the further SAR studies of inhibitors of RNR. The IC_{50} of **1** was determined by Yang and coworkers to be 20 μM. In our experimental setup we obtained an IC_{50} of 139 μM for **1**. This discrepancy is most likely due to differences in the protein production protocol, buffer conditions, and/or protein concentrations in the assay.

To obtain an initial understanding of which amino acids are important for affinity to R1 we performed an alanine scan using **1** as the reference peptide to obtain **5**–**11**. This approach is often used to identify the amino acids, which are important for recognition and the residues that can be substituted to increase potency, metabolic stability, and/or conformational rigidity by cyclization. As seen in Table 5 the IC_{50} values of peptides **5**–**8** and **10** dropped at most by a factor of three as compared to **1**. However, when Trp5 or Phe7 were substituted for Ala (**9** and **11**) all inhibition was lost. This indicates that these two amino acid residues are the most important in the interaction with R1.

Design of the Peptide Library Using FHDoE

In the alanine scan performed above, information about the interaction between individual amino acids is not easily interpreted. To extract some of this information and to further study the importance of individual amino acids, we employed the new multivariate design approach, FHDoE, to design a focused peptide library. One advantage of using this approach is that the

Table 5 Inhibitory potency of peptide analogues obtained from *N*-terminal truncation and alanine scan of the heptapeptide R2 *C*-terminus of *M. tuberculosis* RNR

Peptide		Sequence								Inhibition IC$_{50}$ (µM)[a]	Relative inhibition IC$_{50}$(%)
		1	2	3	4	5	6	7			
1	Ac-	Glu	Asp	Asp	Asp	Trp	Asp	Phe	–OH	139 ± 15[b]	100
2	—	Ac-	Asp	Asp	Asp	Trp	Asp	Phe	–OH	390 ± 53[b]	36
3	—	—	Ac-	Asp	Asp	Trp	Asp	Phe	–OH	1110 ± 170	13
4	—	—	—	Ac-	Asp	Trp	Asp	Phe	–OH	—	—
5	Ac-	Ala	Asp	Asp	Asp	Trp	Asp	Phe	–OH	200 ± 29	70
6	Ac-	Glu	Ala	Asp	Asp	Trp	Asp	Phe	–OH	430 ± 92	32
7	Ac-	Glu	Asp	Ala	Asp	Trp	Asp	Phe	–OH	200 ± 36	70
8	Ac-	Glu	Asp	Asp	Ala	Trp	Asp	Phe	–OH	220 ± 35	63
9	Ac-	Glu	Asp	Asp	Asp	Ala	Asp	Phe	–OH	—	—
10	Ac-	Glu	Asp	Asp	Asp	Trp	Ala	Phe	–OH	310 ± 110	45
11	Ac-	Glu	Asp	Asp	Asp	Trp	Asp	Ala	–OH	—	—

[a] IC$_{50}$ values are given with 95% confidence interval.
[b] IC$_{50}$ values reported by Yang *et al.* are 20 µM (**1**) and 60 µM (**2**) (see Ref. 18).

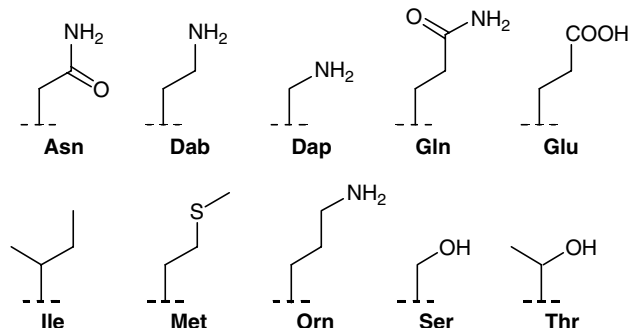**Table 6** Inhibitory potency of peptide analogs from the designed focused library
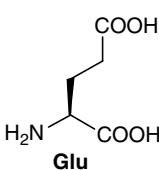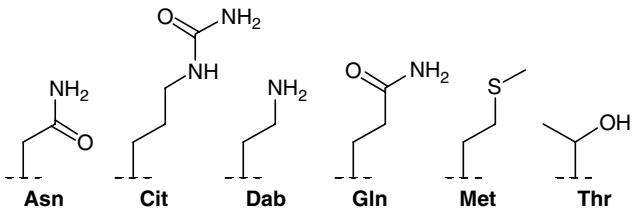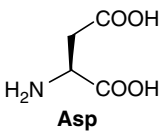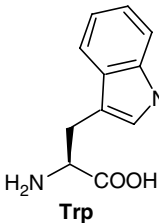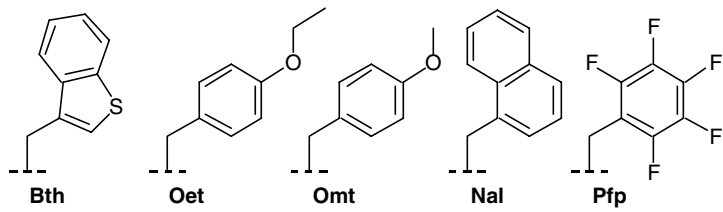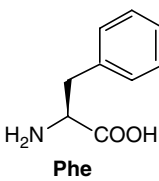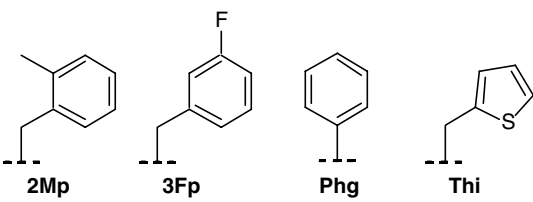
Peptide		Sequence								Inhibition IC$_{50}$ (µM)[a]	Relative Inhibition IC$_{50}$(%)
		1	2	3	4	5	6	7			
12	Ac-	Glu	Asp	Asp	Asp	Trp	Asp	Thi	–OH	250 ± 70	56
13	Ac-	Glu	Asn	Asp	Asp	Omt	Glu	Phe	–OH	—	—
14	Ac-	Glu	Thr	Asn	Asp	Trp	Asp	3Fp	–OH	1310 ± 470	11
15	Ac-	Glu	Asp	Asp	Glu	Trp	Met	Phe	–OH	290 ± 58	48
16	Ac-	Asn	Asp	Met	Ser	Trp	Asp	Phe	–OH	—	—
17	Ac-	Met	Dap	Asp	Asp	Trp	Thr	2Mp	–OH	—	—
18	Ac-	Asn	Asp	Glu	Asp	Trp	Orn	Phg	–OH	—	—
19	Ac-	Thr	Asp	Asp	Orn	Omt	Dab	3Fp	–OH	—	—
20a	Ac-	Glu	Gln	Asp	Dap	Nal	Asp	Phg	–OH	757 ± 240	18
20b	Ac-	Glu	Gln	Asp	Dap	Nal	Asp	Phg	–OH	—	—
21	Ac-	Met	Orn	Asp	Asn	Trp	Asp	Phe	–OH	—	—
22	Ac-	Glu	Ile	Ser	Orn	Trp	Ser	Phe	–OH	—	—
23	Ac-	Dab	Asp	Asp	Asp	Bth	Asp	Phe	–OH	170 ± 30	82
24	Ac-	Glu	Asp	Asn	Asn	Pfp	Asp	Thi	–OH	—	—
25	Ac-	Glu	Asp	Dap	Asp	Oet	Asn	Phe	–OH	—	—
26	Ac-	Cit	Gln	Gln	Glu	Oet	Glu	2Mp	–OH	790 ± 170	18
27	Ac-	Gln	Dab	Met	Asp	Pfp	Asp	Phe	–OH	—	—

[a] IC$_{50}$ values are given with 95% confidence interval.

peptide libraries generated, are biased toward the reference peptide, and thereby increases the probability of retaining potency in the designed peptides. Based on this approach, residues in each position in the reference peptide (**1**) were substituted with residues of similar size and hydrophobic/hydrophilic properties. Since the reference peptide in our case contains as many as five negatively charged side chains, and

the alanine scan showed that they were all possible to substitute for neutral side chains, we were also interested in studying the possibility of replacing these with positively charged residues. Therefore no restriction was placed on the formal charge of each residue and only structural similarity was considered. For example, Glu was substituted with Asn, Cit, Dab, Gln, Met, and Thr (Table 7). In total 16 peptides were

Table 7 Amino acid residues included in the design of the peptide library using FHDoE

Amino acid residues of peptide **1**	Selected amino acid residue side chains from FHDoE

designed and synthesized. The substitutions included coded amino acids as well as noncoded amino acids and the total charge of the peptides ranged from −6 to −3.

SAR of Heptapeptide 1

Results from the alanine scan indicated that side chains in positions 5 and 7 are important for retaining activity. Interestingly, evaluation of the designed peptides showed that there is room for small modifications of these residues. Peptide **23,** in which Trp was replaced by Bth (Table 6), exhibits potency comparable to **1**. Furthermore, in **23** the negatively charged Glu residue in position 1 has been substituted with a positively charged Dab residue. Most likely this position is not

important in the binding with the R1 subunit since the hexapeptide (**2**) which lacks Glu in position 1, is also quite potent. Another observation is that peptides **26** and **20a**, in which the overall net charge of the peptides are reduced from −6 in **1** to −3 have measurable, although low, potencies. Notably, in peptide **26** all the amino acids of **1** have been substituted. Finally, replacement of the *C*-terminal Phe residue in **1**, with the Thi residue, leads to peptide **12** with only a small change in potency.

A QSAR model was developed based on the heptapeptide analogues (**1** and **5**–**27**) using OPLS–DA [21–23]. A final two-component OPLS model was derived that explained 75% of the variation in the responses (R^2Y) with an internal predictability of 0.45 as determined from cross validation. Only one false positive prediction
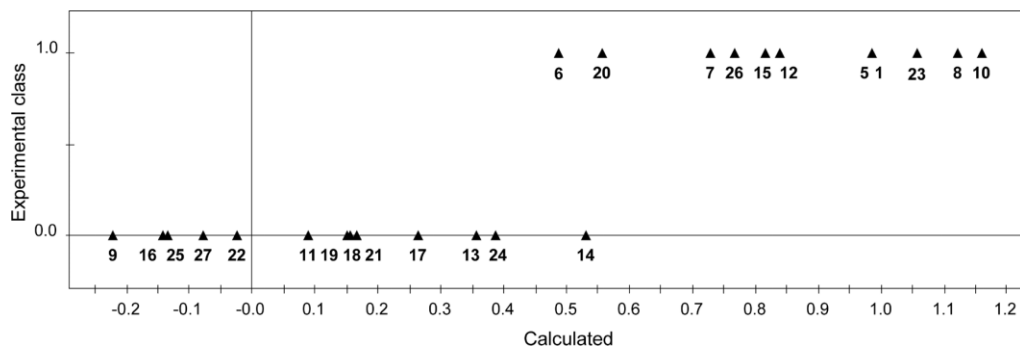
Figure 4 Observed *versus* calculated plot for the discriminative model.

was observed (cut-off = 0.46), peptide 14, which has a measurable, but very low, potency (Figure 4).

The loading plot in Figure 5 indicates that a negative charge in position 3 (negative contribution from p3ch) is beneficial for inhibitory potency, it also seems that a negative charge is preferred in positions 2 and 6. Furthermore, the presence of large side chains in position 5 (positive contribution from p5tciz1) is likely advantageous for potency. Finally, it should be noted that the peptide library was based on a screening design that supports linear terms, and therefore the interaction terms should be treated with caution.

Rationalization of SAR Based on the X-ray Structure of *Salmonella typhimurium* RNR

The RNR of *M. tuberculosis* has high sequence identity to its *Salmonella typhimurium* counterpart. A recent 4 Å X-ray structure of the RNR holoenzyme of *S. typhimurium* [32] (PDB code 2BQ1) suggests that Trp317 of the *C*-terminal R2 subunit (corresponding to Trp5 in **1**) is located in a hydrophobic area close to Phe297, Phe351, Ile681 and Trp684 of the R1 subunit.
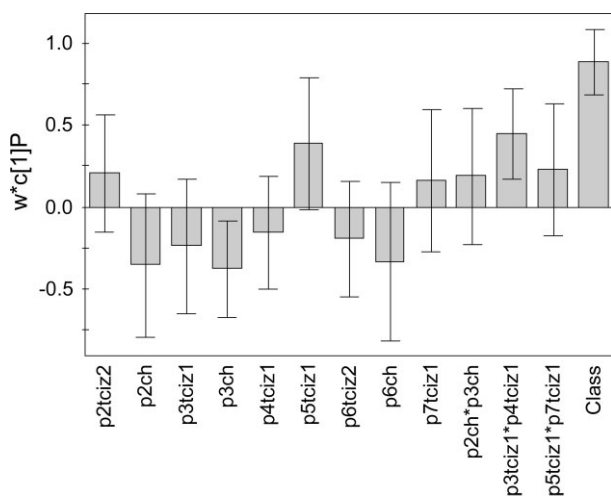

Figure 5 Loading plot of the predictive component shown at 95% confidence intervals. It is seen that large substituents are beneficial in position 5, together with negative charges in position 2, 3 and 6.

A bulkier and more hydrophobic side chain could be accommodated in this pocket, consistent with the derived model term (p5tciz1). In addition, the alanine scan showed that the Phe7 residue was important for inhibitory potency. There is a possible π-cation interaction in the crystal structure between Arg685 and the *C*-terminal Phe residue of the R2 subunit (corresponding to Phe7 in **1**). The density of the Arg685 side chain is poorly resolved but since this interaction cannot be present in **11**, it might explain the drop in potency. All the above mentioned residues in the *S. typhimurium* R1 are conserved in *M. tuberculosis* R1. It was interesting to note that the OPLS coefficients derived from the FHDoE approach could be supported by the structural comparison.

CONCLUSIONS

In summary, a series of peptides based on an *N*-terminal truncation, an alanine scan and a SMD approach were synthesized. The peptides were tested in an RNR activity assay which revealed that Trp5 and Phe7 are important for inhibition and that there may be room for modifications in these positions. A QSAR model was developed based on the synthesized peptides that showed that a negative charge in positions 2, 3, and 6 is beneficial for inhibitory potency. Finally, in positions 5 the model coefficients indicate that there is room for a larger side chain, as compared to Trp5, which is also supported from inspection of the *S. typhimurium* complex structure.

REFERENCES

1. World Health Organization Home Page. http://www.who.int [last accessed Apr 2007].

2. World Health Organization Home Page. http://www.who.int/media centre/factsheets/fs104/en/print.html [last accessed Apr 2007], Fact sheet No 104, March 2007.

3. Thelander L, Reichard P. Reduction of ribonucleotides. *Annu. Rev. Biochem.* 1979; **48**: 133–158.

4. Reichard P. From RNA to DNA, why so many ribonucleotide reductases? *Science* 1993; **260**: 1773–1777.

5. Eriksson M, Uhlin U, Ramaswamy S, Ekberg M, Regnström K, Sjöberg BM, Eklund H. Binding of allosteric effectors to ribonucleotide reductase protein R1: reduction of active-site cysteines promotes substrate binding. *Structure* 1997; **5**: 1077–1092.

6. Larsson A, Sjöberg BM. Identification of the stable free radical tyrosine residue in ribonucleotide reductase. *EMBO J.* 1986; **5**: 2037–2040.

7. Cerqueira NM, Pereira S, Fernandes PA, Ramos MJ. Overview of ribonucleotide reductase inhibitors: an appealing target in anti-tumour therapy. *Curr. Med. Chem.* 2005; **12**: 1283–1294.

8. Wnuk SF, Robins MJ. Ribonucleotide reductase inhibitors as anti-herpes agents. *Antiviral Res.* 2006; **71**: 122–126.

9. Cole ST, Brosch R, Parkhill J, Garnier T, Churcher C, Harris D, Gordon SV, Eiglmeier K, Gas S, Barry CE III, Tekaia F, Badcock D, Basham D, Brown D, Chillingworth T, Connor R, Davies R, Devlin K, Feltwell T, Gentles S, Hamlin N, Holroyd S, Hornsby T, Jagels K, Krough A, McLean J, Moule S, Murphy L, Oliver K, Osborne J, Quail MA Rajandream MA, Rogers J, Rutter S, Seeger K, Skelton J, Squares R, Squares S, Sulston JE, Taylor K, Whitehead S, Barrell BG. Deciphering the biology of *Mycobacterium tuberculosis* from the complete genome sequence. *Nature* 1998; **393**: 537–544.

10. Dawes SS, Warner DF, Tsenova L, Timm J, McKinney JD, Kaplan G, Rubin H, Mizrahi V. Ribonucleotide reduction in *Mycobacterium tuberculosis*: function and expression of genes encoding class Ib and class II ribonucleotide reductases. *Infect. Immun.* 2003; **71**: 6124–6131.

11. Sassetti CM, Boyd DH, Rubin EJ. Genes required for mycobacterial growth defined by high density mutagenesis. *Mol. Microbiol.* 2003; **48**: 77–84.

12. Climent I, Sjöberg BM, Huang CY. Carboxyl-terminal peptides as probes for *Escherichia coli* ribonucleotide reductase subunit interaction: kinetic analysis of inhibition studies. *Biochemistry* 1991; **30**: 5164–5171.

13. Yang FD, Spanevello RA, Celiker I, Hirschmann R, Rubin H, Cooperman BS. The carboxyl terminus heptapeptide of the R2 subunit of mammalian ribonucleotide reductase inhibits enzyme activity and can be used to purify the R1 subunit. *FEBS Lett.* 1990; **272**: 61–64.

14. Gaudreau P, Michaud J, Cohen EA, Langelier Y, Brazeau P. Structure-activity studies on synthetic peptides inhibiting herpes simplex virus ribonucleotide reductase. *J. Biol. Chem.* 1987; **262**: 12413–12416.

15. Pender BA, Wu X, Axelsen PH, Cooperman BS. Toward a rational design of peptide inhibitors of ribonucleotide reductase: structure-function and modeling studies. *J. Med. Chem.* 2001; **44**: 36–46.

16. Gaudreau P, Brazeau P, Richer M, Cormier J, Langlois D, Langelier Y. Structure-function studies of peptides inhibiting the ribonucleotide reductase activity of herpes simplex virus type I. *J. Med. Chem.* 1992; **35**: 346–350.

17. Moss N, Deziel R, Adams J, Aubry N, Bailey M, Baillet M, Beaulieu P, DiMaio J, Duceppe JS, Ferland JM, Gauthier J, Ghiro E, Goulet S, Grenier L, Lavallee P, Lepine-Frenette C, Plante R, Rakhit S, Soucy F, Wernic D, Guindon Y. Inhibition of herpes simplex virus type 1 ribonucleotide reductase by substituted tetrapeptide derivatives. *J. Med. Chem.* 1993; **36**: 3005–3009.

18. Yang F, Curran SC, Li LS, Avarbock D, Graf JD, Chua MM, Lu G, Salem J, Rubin H. Characterization of two genes encoding the *Mycobacterium tuberculosis* ribonucleotide reductase small subunit. *J. Bacteriol.* 1997; **179**: 6408–6415.

19. Barlos K, Gatos D, Kallitsis J, Rapaphotiu G, Sotiriu P, Wenging Y, Schäfer W. Darstellung geschützter peptid-fragmente unter einsatz substituierter triphenylmethyl-harze. *Tetrahedron Lett.* 1989; **30**: 3943–3946.

20. Muthas D, Lek PM, Nurbo J, Karlén A, Lundstedt T. Focused hierarchical design of peptide libraries – follow the lead. *J. Chemometrics* (in press). DOI: 10.1002/cem.1069.

21. Bylesjö M, Rantalainen M, Cloarec O, Nicholson JK, Holmes E, Trygg J. OPLS discriminant analysis: combining the strengths of PLS-DA and SIMCA classification. *J. Chemom.* in press, DOI: 10.1002/cem.1006.

22. Wold S, Sjöström M, Eriksson L. PLS-regression: a basic tool of chemometrics. *Chemom. Intell. Lab. Syst.* 2001; **58**: 109–130.

23. Trygg J, Wold S. Orthogonal projections to latent structures (O-PLS). *J. Chemom.* 2002; **16**: 119–128.

24. Engström Y, Eriksson S, Thelander L, Åkerman M. Ribonucleotide reductase from calf thymus. Purification and properties. *Biochemistry* 1979; **18**: 2941–2948.

25. Cohen EA, Gaudreau PPB, Langelier Y. Specific inhibition of herpesvirus ribonucleotide reductase by a nonapeptide derived from the carboxy terminus of subunit 2. *Nature* 1986; **321**: 441–443.

26. Cornish-Bowden A. *Fundamentals of Enzyme Kinetics*. Portland Press: London, 2004.

27. Hellberg S, Sjöström M, Skagerberg B, Wold S. Peptide quantitative structure-activity relationships, a multivariate approach. *J. Med. Chem.* 1987; **30**: 1126–1135.

28. Sandberg M, Eriksson L, Jonsson J, Sjöström M, Wold S. New chemical descriptors relevant for the design of biologically active peptides. A multivariate characterization of 87 amino acids. *J. Med. Chem.* 1998; **41**: 2481–2491.

29. Linusson A, Wold S, Norden B. Statistical molecular design of peptoid libraries. *Mol. Divers.* 1998; **4**: 103–114.

30. Andersson PM, Lundstedt T. Hierarchical experimental design exemplified by QSAR evaluation of a chemical library directed towards the melanocortin 4 receptor. *J. Chemom.* 2002; **16**: 490–496.

31. Smith GG, Sivakua T. Mechanism of the racemization of amino acids. Kinetics of racemization of arylglycines. *J. Org. Chem.* 1983; **48**: 627–634.

32. Uppsten M, Färnegårdh M, Domkin V, Uhlin U. The first holocomplex structure of ribonucleotide reductase gives new insight into its mechanism of action. *J. Mol. Biol.* 2006; **359**: 365–377.